DETERMINATION OF RAYLEIGH AND LAMB WAVE VELOCITIES IN DIAMOND FILMS USING AN ACOUSTIC MICROSCOPE

J. C. Johnson and R. B. Thompson
Center for NDE
Iowa State University
Ames, IA 50011

Eric E. Jamieson
Allied-Signal Aerospace Company
Kansas City Division
Kansas City

INTRODUCTION

Acoustic microscopy is a powerful method of determining acoustic surface wave velocities with high spatial resolution. This paper describes the use of an acoustic microscope to measure these velocities in polycrystalline diamond films. Acoustic waves in diamond have a relatively high velocity and that affects the choice of the lens diameter and focal length. A general guideline will be given to determine the type of lens needed. The velocities measured in three diamond films were found to vary greatly depending on the film thickness. In two of the films it was found that Lamb modes rather than leaky Rayleigh waves were generated. After correcting for the associated dispersion, the measured velocities were found to deviate from the Lamb and Rayleigh velocities calculated from the single crystal elastic constants. The possibility for using these deviations to characterize the films will be discussed.

ACOUSTIC MICROSCOPE BACKGROUND

Figure 1 shows an immersed, defocused acoustic microscope. The acoustic signals of interest are the specular reflection which travels along the axis of the spherical lens (ray 1) and the leaky Rayleigh wave (ray 2) which is induced at the critical angle θ_R. The Rayleigh wave velocity is found from the difference between the time of flight of the specular reflection (t_1) and the time of flight of the leaky Rayleigh wave (t_2) for a series of transducer lift-offs (ζ). This method of measuring the Rayleigh wave velocity has high spatial resolution, is cheap and portable and has an accuracy of 10^{-3} or better.

The transducer lift-off can be determined from the stepping motor or from the time of flight of the specular reflection and the velocity of sound in the couplant. Here, the latter method was employed. The time of flight between the two acoustic signals was determined by choosing a particular zero crossing for each and measuring the time between them for each lift-off. ζ vs. Δt was plotted and the slope (m) was used to calculate the Rayleigh wave velocity as shown in Equation (1).

Review of Progress in Quantitative Nondestructive Evaluation, Vol. 14
Edited by D.O. Thompson and D.E. Chimenti, Plenum Press, New York, 1995

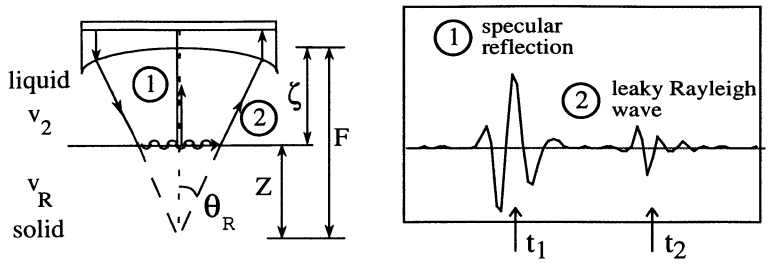

Figure 1. Acoustic microscope and typical signal

$$\frac{V_R}{V_2} = \left[\frac{1}{\left(\frac{m}{V_2}\right)} - \frac{1}{4\left(\frac{m}{V_2}\right)^2} \right]^{-1/2} \qquad (1)$$

Here, V_R is the Rayleigh velocity and V_2 is the velocity in the couplant (water). The error in the Rayleigh wave velocity (σ_{V_R}) was found from the scatter in the slope. The details of the development of this method are given in Johnson and Thompson [1, 2]

DIAMOND FILM BACKGROUND

Diamond films are currently a popular topic for scientific research. Diamond is currently used to coat cutting tools but it could also be used as a protective coating for a variety of materials and products. The protective as well as lubricating aspects of diamond film could be used on everything from ball bearings to cooking pots. Transparent diamond could also protect eyeglasses, watch crystals and computer hard disks. In the electronics industry, diamond would be an exceptional heat sink since it is an an excellent heat conductor, electrical insulator and is unreactive except at high temperatures.[3].

The three polycrystalline diamond films used in this study were grown with a chemical vapor deposition process. They were nominally 100μ, 300μ and 500μ thick. The thinnest of the films had an area of 1 cm by 1 cm and the other two had an area of 0.5" by 0.5". All were free standing with no substrate.

LENS SELECTION

At previous QNDE meetings, Rayleigh wave velocities on the order of 6 mm/μs have been reported in silicon nitride (Si_3N_4) [1, 2] using a 50 MHz transducer with a diameter of 0.25" and a focal length of 5 mm. The leaky Rayleigh wave signals seen in the diamond films with this lens had small amplitude and were imbedded in the specular reflection even when the microscope was completely defocused. Figure 2 is a sketch of the lens as seen from the side and top. The left side shows the angular extent of half the lens (40°), the critical angles to induce leaky Rayleigh waves for Si_3N_4 (θ_R=15°) and for diamond (θ_R=8°). The incident energy which produces the leaky Rayleigh wave is roughly proportional to the area on the surface of the lens defined by $d\theta$ at θ_R. The right side of figure 2 shows these areas for diamond (inner ring) and for Si_3N_4 (outer ring). The area, and therefore the energy, of the ring for Si_3N_4 is much larger than the area of the ring for diamond. For this reason the Rayleigh wave signal produced with this lens for Si_3N_4 was stronger than for diamond. Also, the time delay between the leaky Rayleigh wave and the specular reflection for diamond are similar. Therefore the Rayleigh wave remained imbedded within the specular reflection when the transducer was defocused.

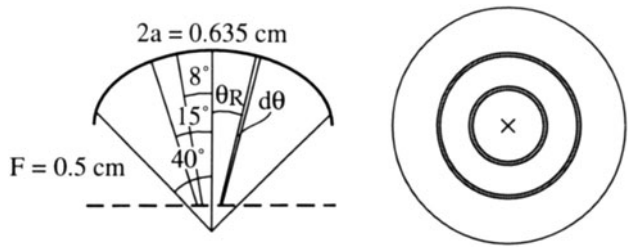

Figure 2. Acoustic microscope lens (seen from the side and top) with critical angles for silicon nitride (15°) and diamond (8°).

Figure 3 shows a sketch of the transducer lens used successfully on the diamond films. This transducer also had a frequency of 50 MHz and a diameter of 0.25" but the focal length was 0.5". Due to the longer focal length the angle between the axis and the edge of the lens was only 15°. In this case the critical angle for diamond of 8° was a much larger fraction of axis-edge angle so the area of the ring defined by dθ was much larger than with the previous lens. Therefore, the Rayleigh wave signal was much stronger. Also, the time delay between the Rayleigh wave signal was much larger than that of the specular reflection so it was possible to resolve the two signals in time over a range of transducer lift-offs. A general guideline to avoid these problems is to choose the diameter and the focal length of the transducer for the sample in question so that the critical angle is somewhat larger than one half the angle between the axis and the edge of the lens.

Typical signals with the second lens and the three diamond films (not at the same lift-off) are shown in Figures 4a), b) and c). Two separate signals can be seen in each figure. The first signal is the specular reflection and the second was assumed initially to be the leaky Rayleigh wave. There are more oscillations per signal in figure 4 than in the typical signal shown in figure 1 since the second transducer was not as highly damped as the previous one.

The zero crossings used to calculate the velocity are marked with an x. They were chosen to allow the greatest range of lift-off and to avoid interference. In order to have the greatest range of ζ, it was advantageous to have the zero crossing later in the second signal. However, the 300μ film (figure 4b) shows signal interference of at least two frequencies. In order to avoid the interference, the zero crossing was chosen early in the second signal.

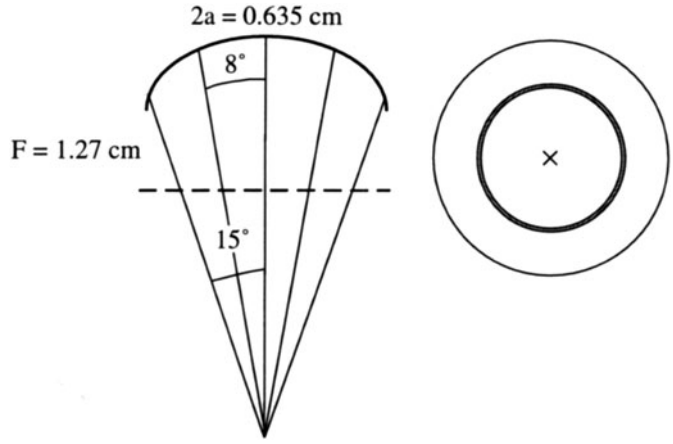

Figure 3. New lens selected for the diamond films

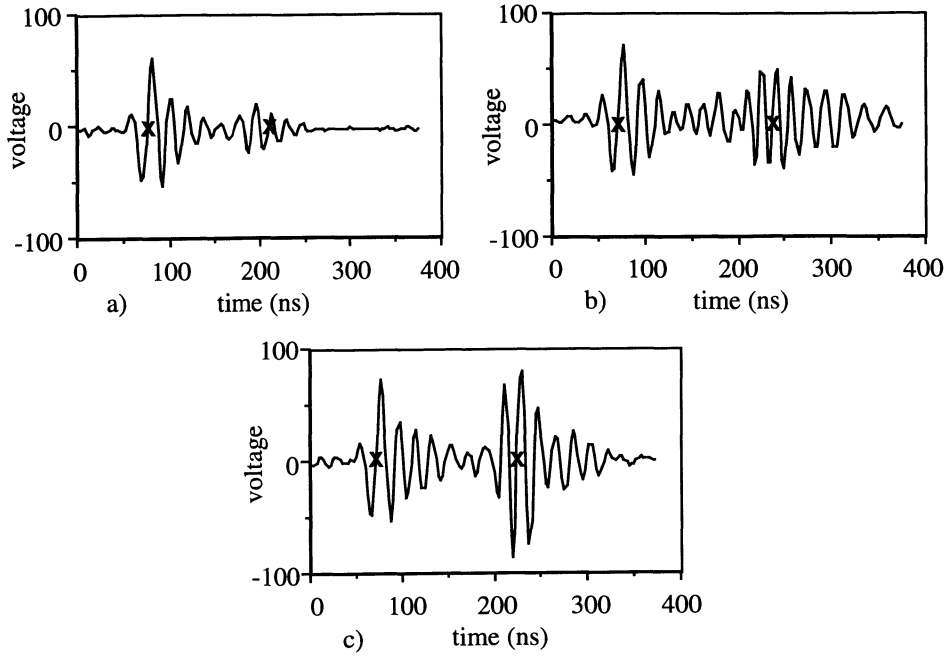

Figure 4. The front surface and the surface wave signals from the a) 100μ diamond film, b) 300μ diamond film and c) 500μ diamond film.

WAVE VELOCITY

The velocities for the three films are given in Table 1 along with the thicknesses in wavelengths at the nominal center frequency of 50 MHz. The error quoted in the velocity is due to the scatter in the plot of ζ vs Δt as described previously. There are two items of note in the data. First, there is a large difference between the acoustic wave velocity as measured in the 100μ film and the velocities from the other two. Second, the uncertainty in velocity in the 300μ film is much larger than other two. This is due to the interference described above.

The Rayleigh wave velocity for diamond can be estimated from Poisson's ratio as shown in equation (2).

$$V_R \cong \frac{0.87 + 1.12\sigma}{1 + \sigma} V_T = 10.7 \text{ mm/}\mu\text{s} \qquad (2)$$

Here σ is Poisson's ratio and is approximately 0.09 and V_T is the shear velocity and is approximately 12 mm/μs [4]. The estimated velocity of 10.7 mm/μs is similar to the velocities measured for the 300 and the 500μ films. From this calculation, the acoustic wave measured in the 100μ film cannot be a Rayleigh wave.

Table 1. The measured acoustic wave velocities and uncertainties for the three diamond films

100 μ	0.5 λ	8.77 ± 0.01 mm/μs
300 μ	1.6 λ	10.4 ± 0.2 mm/μs
500 μ	2.6 λ	10.81 ± 0.04 mm/μs

LAMB WAVES

The acoustic wave measured in the 100μ film is properly interpreted as a Lamb wave. Lamb waves occur in plates as longitudinal and vertically polarized shear waves, bouncing between the surfaces, couple at the boundaries. There are two modes, symmetric and antisymmetric. Both have a zeroth and higher modes of vibration and both are dispersive. The velocities of these waves are calculated from the dispersion curves which are the solutions to the Rayleigh-Lamb frequency equations [5].

The dispersion curves were calculated from the single order elastic constants for diamond. They are c_{11}=1040 GPa, c_{44}=550 GPa and c_{12}=170 GPa [4]. The Voigt averaging procedure [6] was used to convert these values into polycrystalline Lamé constants. This assumes that there is no texture in the films. In principle, Reuss and Hill procedures should also be considered. However, they were not pursued in this initial study because of significant uncertainty in the second order constants c_{IJ}, as much as 30% for c_{12}. The Lamé constants along with the film thickness and density were used to obtain solutions to the Rayleigh-Lamb frequency equations [5]. These solutions are the dispersion curves shown in Figures 5a), b) and c).

The axes of the graphs in figure 5 are frequency (MHz) vs. wave vector (mm^{-1}). An x marks the measured velocity. The dashed lines represent the ± errors in the velocity given in Table 1. For the 100μ and the 500μ plots, the dashed lines cannot be resolved on the scale given. The zeroth order symmetric and antisymmetric modes are labeled (s_o and a_o, respectively) in all three plots. Higher order modes are not labeled to avoid confusion. At high frequency and wave vector, the a_o and s_o modes approach an asymptotic limit which has a slope proportional to the Rayleigh wave velocity. This line is shown for the 100μ curve but is left off the 300μ and the 500μ curve in the interest of clarity.

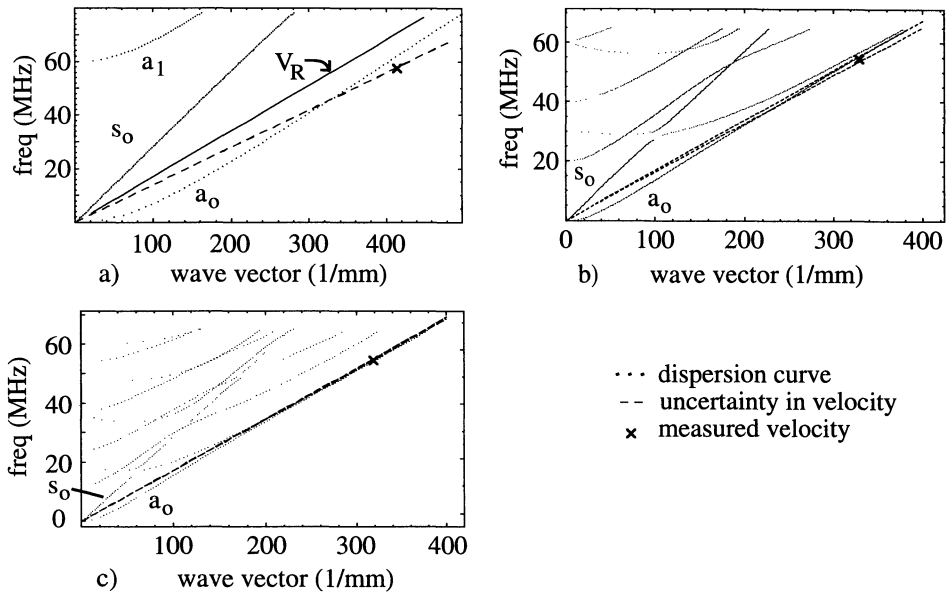

Figure 5. The dispersion curves and experimentally determined velocity (marked with an x) for the a) 100μ, b) 300μ and c) 500μ diamond films.

The type of wave generated in the films can be determined by comparing the experimental velocity to the dispersion curves in figure 5. From figure 5a), the point representing the experimental velocity measured in the 100μ film is closest to that of the zeroth order antisymmetric Lamb wave and is further from the line representing the Rayleigh wave velocity. This is why the measured velocity (8.77 mm/μs) did not agree with the estimated Rayleigh wave velocity (10.7 mm/μs). The relatively good agreement between the measured velocity for the 500μ diamond film and the estimated Rayleigh velocity can be seen from figure 5c where the x can be considered to be on the asymptotic limit described above. The point representing the measured velocity for the 300μ film (figure 5b) lies near both the a_o and s_o curves but not near where they converge to a Rayleigh wave mode. The interference can be explained by the presence of both a_o and s_o modes in the film.

The experimental velocities lie near the theoretical dispersion curves but there are deviations in all three cases. The largest is seen in figure 5a). The point representing the measured velocity lies somewhat below the a_o curve. One explanation for deviation would be a difference between the nominal and the actual film thickness; which in turn, influences the dispersion curves. The thickness of the diamond films was checked and the correct thicknesses were found to be 97.5±10μ, 284±20μ and 463±25μ. Figures 6a), 6b) and 6c) show new dispersion curves with the correct thickness. In this case, only a localized region near the measured velocity point and the a_o curve are shown. There are two sets of dashed lines. One set represents the uncertainty in the thickness given above and the other represents the uncertainty in the velocity given earlier. For figure 6c) the dashed lines representing the uncertainty in the thickness are very difficult to perceive because they lie very close to the dispersion curve. The point representing the measured velocity is above the dispersion curve in figure 6c) which is difficult to explain. In figure 6b) the point representing the measured velocity is below the corrected dispersion curve but the large uncertainty in the velocity makes it difficult to claim any sort of trend.

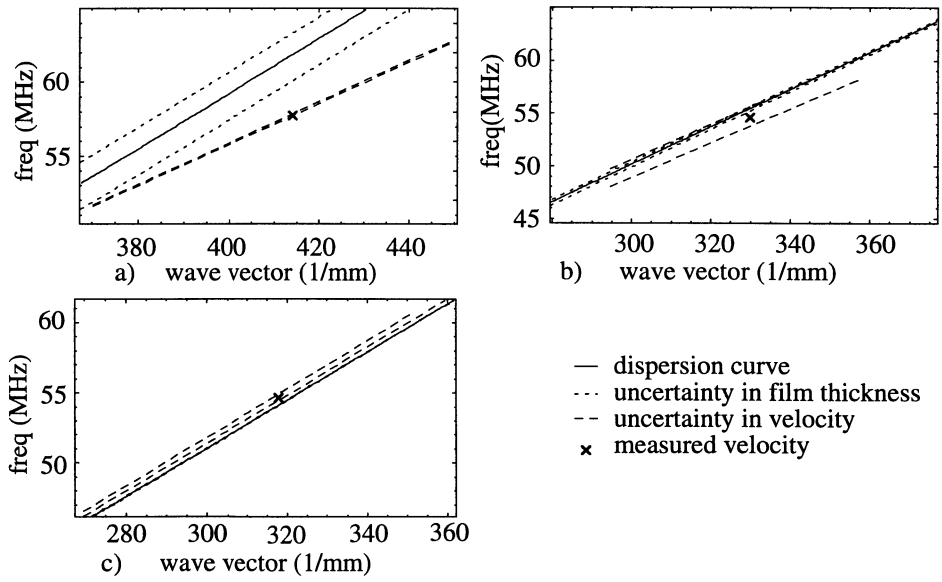

Figure 6 Corrected dispersion curves for the three diamond films. a) 97.5±10μ, b) 284±20μ and c) 463±25μ.

However, the measured velocity is low with respect to the s_0 mode (shown in figure 5b) which is assumed to be present due to the interference observed. In figure 6a) which is the corrected dispersion curve for the thinnest film, there is no doubt that there is a deviation between the theoretical and the experimental values. Here the regions of uncertainty do not overlap and the point definitely lies below the dispersion curve.

Two possible explanations for the deviations are texture and film composition, the latter of which will be discussed here. A film that is not 100% diamond but is mixed with some other form of carbon such as amorphous carbon or graphite can be expected to have a different acoustic wave velocity. Figure 7 shows the previous dispersion curves for pure diamond, pure graphite, a mixture of the two and the point representing the measured velocity. The Lamé constants for graphite were estimated from the single crystal elastic constants (for a hexagonal crystal in this case) [4] with a Voigt averaging procedure [6]. There is good agreement between the experimental velocity and the curve for the diamond-graphite mixture. The film content must be checked independently to confirm these results but these results suggest that acoustic wave velocities could be used to test the purity of diamond films.

CONCLUSION

In order to measure wave velocities with an acoustic microscope, careful consideration must be given to the choice of the combination of lens diameter and focal length. The wave velocity and therefore the critical angle is sample dependent. If the angle between the axis of the lens and it's edge is too small, no surface wave will be produced. If the angle is too large, the wave will have a small amplitude and may be imbedded in the specular reflection. As a general rule, choosing the lens such that the critical angle for the material is somewhat greater than one half the axis-edge of lens angle appears to yield best results.

Acoustic microscopy can be used to measure acoustic wave velocity in thin films. The waves produced are either Rayleigh waves or Lamb waves depending on the frequency and the film thickness. For films that are much thicker than the acoustic wavelength, Rayleigh waves are produced. For films which have thicknesses less than or equal to the wavelength, Lamb waves are produced.

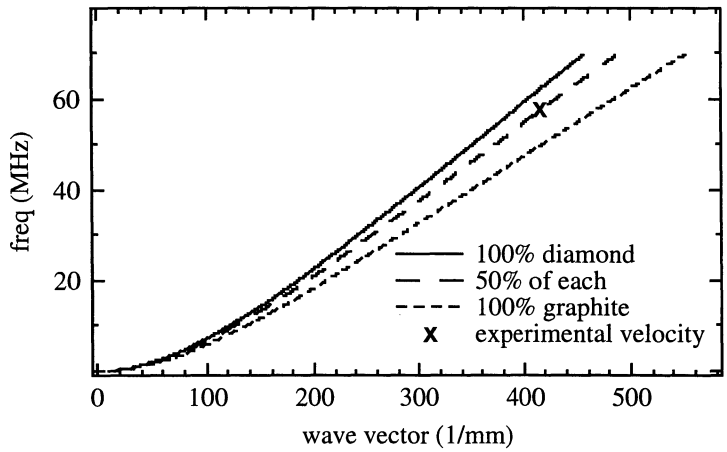

Figure 7 The a_0 dispersion curve for diamond, graphite and a mixture of the two.

The velocities measured showed deviation from that predicted from the bulk diamond constants. Possible explanations for this are texture or the existence of other forms of carbon in the film. A diamond-graphite mixture would have a similar velocity to the measured velocity. Future work includes independent analysis of the films by Raman spectroscopy to check their content. If the films are found to be mostly diamond then the texture will have to be investigated.

REFERENCES

1. J. Johnson and R. B. Thompson, in *Review of Progress in Quantitative NDE*, Vol. 12, edited by D. O. Thompson and D. E. Chimenti (Plenum Press, New York, 1993), p. 2121.
2. J. Johnson and R. B. Thompson, in *Review of Progress in Quantitative NDE*, Vol. 13, edited by D. O. Thompson and D. E. Chimenti (Plenum Press, New York, 1994), p. 2017.
3. Ivan Amato. in *Science News*, Vol. 138, (1990), p.72.
4. K.-H. Hellwege, Landolt and Bernstein: *Numerical Data and Functional Relationships in Science and Technology*, Group III, Vol. 11, (Springer-Verlog, Berlin, 1979), pg. 9.
5. B. Auld., *Acoustic Waves and Fields on Solids*, Wiley Interscience, New York, NY, 1973, Ch. 10.
6. W. Voigt, *Lerbuch der Kristallphysik*, Taubner, Leipzig, 1928.